American Mineralogist
Vol. 57, pp. 1260–1271 (1972)

DETERMINATION OF LIQUIDUS RELATIONS IN SYNTHETIC SILICATE SYSTEMS WITH ELECTRON PROBE ANALYSIS: THE SYSTEM FORSTERITE–DIOPSIDE–SILICA AT 1 ATMOSPHERE

IKUO KUSHIRO, *Geophysical Laboratory, Carnegie Institution of Washington, Washington, D. C. 20008*

ABSTRACT

A new method of determining the equilibrium liquidus diagram with the use of electron probe analysis has been applied to the petrologically important system forsterite (Mg_2SiO_4)–diopside ($CaMgSi_2O_6$)–silica at 1 atm and has been found to be very efficient. The analysis shows that the diopside solid solutions in this system have a small amount (less than 5 weight percent) of forsterite component near liquidus temperatures. The analysis has confirmed the incongruent melting of pure diopside that has been used for a secondary standard in the temperature scale, the existence of iron-free pigeonite on the join diopside–enstatite ($MgSiO_3$) between diopside 6 enstatite 94 and diopside 23 enstatite 77 (weight percent) at the solidus, and the nonbinary nature of the joins forsterite–diopside and diopside–silica.

INTRODUCTION

The liquidus relations of many synthetic silicate systems at 1 atm have contributed greatly to the understanding of the crystallization of magmas and the origin of various igneous rocks. Determination of the liquidus surface, which is of prime importance in melting relations, has been made mostly by the "quenching method" (Bowen, 1912) in synthetic silicate systems. By this method mixtures with appropriate compositions are made in a given system and are heated near liquidus temperatures to determine which mineral is the liquidus phase, *i.e.*, the phase that crystallizes first when the temperature is lowered from the all-liquid condition. The liquidus boundaries, which separate the liquidus surfaces of different liquidus phases, are obtained by locating the limits within which a particular phase crystallizes first. This method, however, requires a relatively large number of mixtures as well as a number of runs for accurate determination of the liquidus boundaries.

More direct determination of liquidus boundaries is possible with the use of electron probe analysis of glass (quenched liquid). Since a liquid coexisting with two different solid phases, for example, lies on the liquidus boundary, the analysis of the glass quenched from such liquid gives the location of the liquidus boundary. Similarly, the composition of the liquid coexisting with three different solid phases gives the junction of three liquidus phase boundaries or an isobaric invariant point in a ternary system. In the present study, this method is applied to the system forsterite–diopside–silica at 1 atm, which has been studied by Bowen (1914), Schairer and Yoder (1962), Boyd and Schairer (1964), and Kushiro and Schairer (1963). Twenty-two run products were selected from among the runs made by the above investigators, and glass and coexisting crystals have been analyzed with the Material Analysis Company electron probe. The method of analysis and correction procedures are the same as those described by Bence and Albee (1968), Boyd (1968), and Finger and Hadidiacos (1971).

RESULTS OF ANALYSIS AND DISCUSSION

The results of the electron probe analysis of glass are given in Table 1, and the compositions are plotted in the system Fo–Di–SiO_2[1] (Fig. 1). The run products selected for this study were held at temperature for 4–120 hours. In most of them the glass is very homogeneous and free of quench crystals, and analyses of different parts of the glass give very similar compositions. Most of the compositions given in Table 1 are the average of two analyses for each run product. The maximum deviations from the average are 0.25, 0.23, and 0.35 weight percent for CaO, MgO, and SiO_2, respectively.

The location of the liquidus boundary between pyroxenes and the silica mineral determined in this study is identical with that determined by Bowen (1914) and Schairer and Yoder (1962). However, the boundaries between Fo_{ss} and pyroxenes determined in this study are located slightly to the silica-rich side of those determined by Schairer and Yoder (1962) and Kushiro and Schairer (1963). This could be due to the difficulty of finding a very small amount of forsterite which might have settled down in the bottom of the containers (thin Pt foil envelopes) in some of the critical runs made in the previous experiments for the mixtures just inside the true forsterite field. The boundary between Di_{ss} and Ca-poor pyroxene (Pi as discussed later), which connects two different isobaric (1 atm) invariant points $Fo_{ss} + Di_{ss} + Pi + L$ and $Di_{ss} + Pi + Tr + L$, also appears to be displaced, although the previous boundary was suggested by the above authors as preliminary. In the present study, however, the glasses in

---

[1] Abbreviations used in this paper: Ak, akermanite; Cr, cristobalite (SiO_2); Di, diopside ($CaMgSi_2O_6$); Di_{ss}, diopside solid solution; En, enstatite ($MgSiO_3$); Fo, forsterite (Mg_2SiO_4); Fo_{ss}, forsterite solid solution; Gl, glass; L, liquid; Pi, iron-free pigeonite; Pr_{ss}, protoenstatite solid solution; Px, pyroxene; Tr, tridymite; Wo, wollastonite ($CaSiO_3$).

TABLE 1. Electron Probe Analyses of Glass Coexisting with More Than Two Different Solid Phases in the System Fo-Di-SiO_2 at 1 Atm

Starting material, weight percent			Temperature, °C	Analyses, weight percent			
Di	Fo	SiO_2		CaO	MgO	SiO_2	Total
Fo_{ss}—Ca-poor Px boundary							
10	65	25	1530	3.70	35.99	62.28	101.97
			1515	6.18	33.65	61.62	101.45
15	85 (En)		1430	13.66	26.30	58.59	98.85
25	75 (En)		1420	15.02	25.36	58.70	99.08
30	50	20	1410	15.52	24.61	58.54	98.67
50	37	13	1390	17.29	23.47	57.85	98.61
Fo_{ss}—Di_{ss} boundary							
75	20	5	1390	20.80	23.46	56.02	100.28
89	11	...	1388.5	23.32	22.47	53.93	99.72
65	25	10	1388	18.23	22.46	57.25	97.95
60	30	10	1388	18.15	23.47	58.57	100.19
89	11	...	1384	24.58	22.09	52.96	99.63
Ca-poor Px (Pi)—Di_{ss} boundary							
64	21.7	14.3	1380	17.30	21.97	59.14	98.41
Ca-poor Px—Cr boundary							
22	45.6	32.4	1505	5.81	29.85	64.31	99.97
37	34.3	28.7	1460	9.51	26.75	64.06	100.32
51	25.2	23.8	1395	14.75	22.17	61.84	98.76
Di_{ss}—Cr boundary							
70	14	16	1373	17.56	20.05	61.68	99.29
85	3.5	11.5	1370	21.79	16.29	61.86	99.94
90	...	10	1367	22.31	13.97	61.84	98.12
			1365	24.18	12.58	60.98	97.74
Fo_{ss}—Ca-poor Px (Pi)—Di_{ss} invariant point							
50	37	13	1385	17.90	23.56	58.22	99.68
60	30	10	1385	17.99	23.62	58.76	100.37
66	22.4	11.6	1385	17.55	23.28	57.82	98.65
Ca-poor Px (Pi)—Di_{ss}—Cr invariant point							
60	21	19	1373	16.83	20.59	61.93	99.35

two different runs at 1373°C give two significantly different compositions, as shown in Figure 1, and the exact position of the invariant point $Di_{ss} + Pi + Tr + L$ is still not certain. Since the glass with lower diopside content clearly coexists with two pyroxenes, Di_{ss} and Pi, and the silica mineral, as confirmed by electron probe analysis, this composition is considered to be at the invariant point, and the boundary has been drawn to connect this composition in Figure 1. The new boundary is, however, still within the limits of compositions given by Schairer and Yoder (1962) and is consistent with the experimental results obtained by them.

On the other hand, another invariant point, $Fo_{ss} + Di_{ss} + Pi + L$, has been determined with relatively high precision. The analyses of glass in three different runs made at 1385°C coincide within 1 percent (in terms of Fo, Di, and SiO_2 relative weight percent). The glass in these runs coexists with Fo_{ss}, Di_{ss}, and Pi as confirmed also by electron probe analysis, indicating the invariant relationship at 1 atm. This invariant point must be a reaction point where Fo reacts with

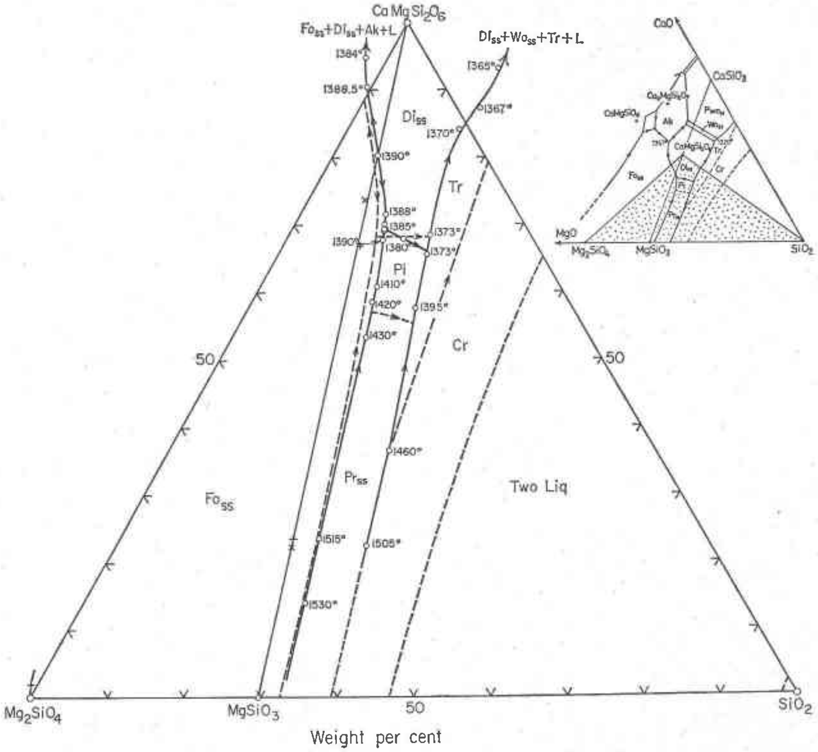

FIG. 1. Liquidus boundaries in the system forsterite–diopside–silica at 1 atm determined by electron probe analysis of glass coexisting with two or more different crystalline phases. Dashed boundaries Bowen (1914), Schairer and Yoder (1962), and Kushiro and Schairer (1963); solid boundaries, this study; crosses, compositions of Fo_{ss}, Di_{ss}, and Pi at 1385°C (1 atm invariant point); X, compositions of Di_{ss} and Pi at 1373°C (another 1 atm invariant point).

liquid, and Di_{ss} and Pi precipitate; that is, the reaction $Fo_{ss} + L \rightleftarrows Di_{ss} + Pi$ takes place.

The glass formed at 1388.5°C from a mixture $Di_{89}Fo_{11}$ (weight percent) has a composition off the system Fo–Di–SiO_2; that is, the glass is deficient in silica when Fo and Di molecules are calculated. This evidence indicates that the join Fo–Di is not binary and not a thermal barrier, as has already been suggested by Kushiro and Schairer (1963). The liquidus boundary between Fo_{ss} and Di_{ss} drops continuously from a maximum, which is slightly to the silica-poor side of the join Di–En, toward the invariant point $Fo_{ss} + Di_{ss} + AK + L$ (1357°C) across the join Fo–Di (Fig. 1). The composition of the liquid just above the solidus (1384°C) for a mixture $Di_{89}Fo_{11}$ has been determined (Table 1, Fig. 1). It is considerably away from the join Fo–Di.

The presence of a maximum on the liquidus boundary between Fo and Di_{ss} has been confirmed by the evidence that the liquid coexisting with Fo_{ss} and Di_{ss} at 1390°C exists near the join Di–En, whereas the liquids at slightly lower temperatures (1388.5° and 1388°C) exist on both the silica-poor and silica-rich sides of the liquid at 1390°C.

The glass formed at 1367° and 1365°C from a mixture on the join Di–SiO_2 also lies off the system Fo–Di–SiO_2. In this case, the composition of the glass is deficient in MgO, and Wo molecule is calculated in addition to Di and silica. This evidence indicates that the join Di–SiO_2 is also not binary and not a thermal barrier, as was also suggested by Schairer and Kushiro (1964). The liquidus boundary between Di_{ss} and a silica mineral drops continuously from the invariant point $Di_{ss} + Pi + Tr + L$ to another invariant point, $Di_{ss} + Tr + Wo + L$ (1320°), across the join Di–SiO_2, although the liquids within the system Fo–Di–SiO_2 never reach it (Fig. 1).

The crystals have also been analyzed (Table 2). They are homogeneous, and no significant compositional variation was detected by electron probe. The limits of diopside and Ca-poor pyroxene (Pi) solid solutions have been determined by analyzing the Di_{ss} and Pi coexisting with Fo_{ss} (0.56 weight percent CaO, 1.6 weight percent monticellite) and glass at the 1 atm invariant point (1385°C). The compositional gap across the two-pyroxene field at the solidus is about 43 weight percent Di, a little (4 percent Di) more extensive than that determined by Boyd and Schairer (1964) by the powder X-ray diffraction technique. The amount of the discrepancy between the X-ray and the electron probe measurements on the position of the solvus is nearly the same as that found by Boyd (1970) in the system Di–En at 30 kb.

The analysis of pyroxenes indicates the existence of two different

TABLE 2. Electron Probe Analyses of Olivine and Pyroxenes in the System Fo-Di-SiO_2 at 1 Atm

Starting material, weight percent			Temperature, °C	Phase	Analyses, weight percent			
Di	Fo	SiO_2			CaO	MgO	SiO_2	Total
5	95 (En)		1470	Ca-poor Px (with cracks)	0.44 (±0.01)	40.39	60.16	100.99
			1400	Ca-poor Px (with cracks)	0.73 (±0.09)	39.63	59.83	100.19
			1400	Ca-poor Px (without cracks)	1.91 (±0.21)	38.79	60.08	100.78
			1365	Ca-poor Px (with cracks)	0.81 (±0.07)	39.13	59.53	99.47
7.5	92.5 (En)		1455	Ca-poor Px (with cracks)	0.51 (±0.02)	39.99	60.06	100.56
10	90 (En)		1425	Ca-poor Px (with cracks)	0.69 (±0.05)	40.17	59.96	100.82
			1425	Ca-poor Px (without cracks)	1.58 (±0.20)	39.41	59.97	100.96
35	65 (En)		1400	Ca-poor Px (without cracks)	3.72 (±0.07)	37.35	59.22	100.29
50	37	13	1390	Ca-poor Px (without cracks)	5.47	35.50	58.86	99.84
			1385	Ca-poor Px (without cracks)	6.09	35.47	59.26	100.84
			1385	Fo_{ss}	0.56	58.25	43.47	102.27
64	21.7	14.3	1380	Ca-poor Px (without cracks)	5.55	35.77	58.58	99.90
			1380	Di_{ss}	17.80	25.98	57.18	100.96
60	21	19	1373	Ca-poor Px (without cracks)	5.79	35.50	58.78	100.06
			1373	Di_{ss}	19.13	24.71	56.08	99.93
89	11	...	1388.5	Di_{ss}	23.79	21.02	55.28	100.09
66	22.4	11.6	1385	Di_{ss}	17.19	25.14	56.88	99.21
90	...	10	1367	Di_{ss}	23.69	20.25	56.36	100.57
75	20	5	1390	Di_{ss}	19.75	23.10	55.36	98.21
				Fo_{ss}	0.95	57.14	43.64	101.73

Numbers in parentheses are the maximum deviations from the average of CaO in Ca-poor Px.

Ca–poor pyroxenes. One is a low–Ca member and the other is a relatively high–Ca member. Careful analysis of the run products made by Boyd and Schairer (1964) has revealed that two different Ca–poor pyroxenes coexist in the runs made at 1425° and 1400°C for compositions $Di_{10}En_{90}$ and Di_5En_{95}, respectively. The difference in CaO content between these two Ca–poor pyroxenes is 0.9 weight percent (3.4 weight percent Di) at 1425°C and 1.2 percent (4.6 percent Di) at 1400°C (Table 2). The compositions in Table 2 are the average of four different analyses for each Ca–poor pyroxene. The maximum deviation from the average of CaO is given for each analysis, since the Ca content is critical in these analyses. The crystals of both the Ca–poor pyroxenes are very large (up to 50 μm) and homogeneous. The low–Ca pyroxene always shows a number of cracks, reported by Boyd and Schairer (1964) in the inverted protoenstatite, whereas the relatively high–Ca pyroxene does not show such cracks; and in many cases they are identified easily on this basis under the microscope, especially if they coexist with glass, *i.e.,* in the runs made above the solidus. Recently, Yang (1971) has identified orthorhombic and monoclinic Ca–poor pyroxenes on the join Di–En at 1 atm by interfacial angle measurement of the synthesized crystals. The former, which would be protoenstatite solid solution, and the latter, which is called "iron–free pigeonite," have different solid solution ranges along the join Di–En with a solvus of about 5 percent Di at 1432°C. Yang (1971) suggests a peritectic relationship between them, the protoenstatite solid solution reacting with liquid to form the iron–free pigeonite at 1432°C. The two different Ca–poor pyroxenes found in the present study are presumed to be protoenstatite solid solution and iron–free pigeonite, respectively. The latter would be essentially the same phase as that synthesized from $Di_{20}En_{80}$ composition by Kushiro (1969) at 20 kb and by Kushiro and Yoder (1970) at lower pressures.

On the basis of the present analyses, the equilibrium diagram of the join Di–En has been constructed (Fig. 2). At 1425°C, Pr_{ss} and Pi coexist with the liquid rich in Di component, indicating that this temperature is that of the peritectic point, where the reaction $Pr_{ss} + L \rightleftarrows Pi$ takes place. This temperature is a little lower ($\sim$7°) than that reported by Yang (1971). The liquidus boundary between Pr_{ss} and Pi in the system $Fo\text{–}Di\text{–}SiO_2$ has been drawn in Figure 1 on the basis of the phase relations along the join Di–En and the optical examination of the run products made by Schairer and Yoder (1962) on the mixtures $Di_{55}En_{32}silica_{13}$, $Di_{58}En_{37}silica_{5}$, $Di_{58}En_{28}silica_{14}$, $Di_{60}En_{30}silica_{10}$, and $Di_{60}En_{27}silica_{13}$. The near–liquidus runs for the first two mixtures appear to have Pr_{ss} as the liquidus phase, whereas the others have Pi. The Pr_{ss} has a solid solution range at least up to 2.8 percent Di at 1400°C. The solid solution range may increase with lowering temperature until Pi becomes unstable (Fig. 2). The solid solution range of Pi is very wide near the solidus, *i.e.,* 15 percent Di at 1385°C. The limit of the solid solution of Pi at 1385°C is exactly the same as that of clinopyroxene solid solution determined by Boyd and Schairer (1964). By extrapolating the two–pyroxene region between Pr_{ss} and Pi at 1400° and 1425°C, it would be expected that the Pi field terminates at a temperature between 1200° and 1300°C as shown in Figure 2.

The results of the present study, based on microprobe analysis, have made a significnat addition to the phase equilibrium relations suggested by Boyd and Schairer (1964), which are based on optical and powder X–ray techniques.

In the light of these results, it would be desirable to study the iron-bearing system, *i.e.*, (Mg, Fe)SiO_3–Ca(Mg, Fe)Si_2O_6, with variable Fe/Mg ratio at 1 atm to determine if the pigeonite field extends toward iron–rich compositions and is separated by a two–pyroxene region from the fields of protoenstatite and orthopyroxene solid solutions (or high clinohypersthene with $C2/c$ symmetry).

Analyses have also been made on Di_{ss} formed near the liquidus temperatures (1390° ~ 1392°C) for the compositions $Di_{80}En_{20}$, $Di_{85}En_{15}$, $Di_{90}En_{10}$, and $Di_{95}En_5$ as well as pure Di (Table 3) to confirm the presence of the liquidus maximum near $Di_{90}En_{10}$ (Kushiro and

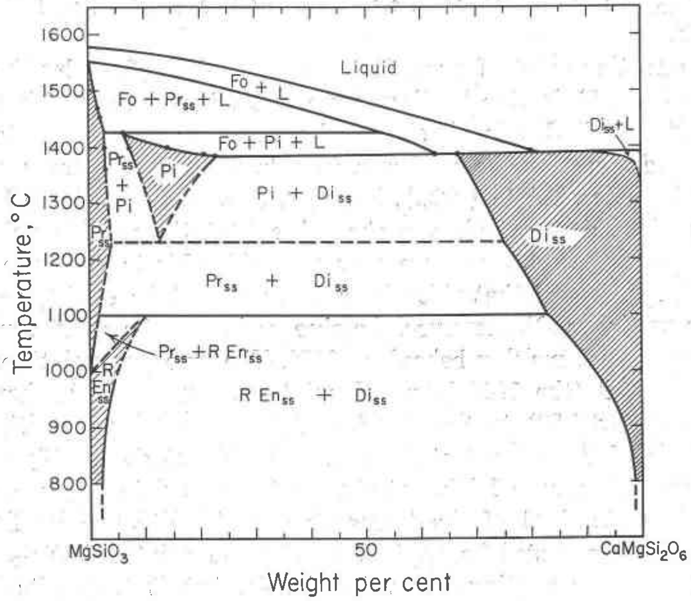

FIG. 2. Revised equilibrium diagram of the join $MgSiO_3$–$CaMgSi_2O_6$ at 1 atm. Original diagram by Boyd and Schairer (1964). Fo in this system is forsterite solid solution containing CaO up to about 0.6 percent. The melting interval of Di_{ss} near $CaMgSi_2O_6$ is exaggerated (see Fig. 4).

Schairer, 1963). The analyses show that the compositions of all these Di_{ss} do not lie on the join Di–En, but lie between the joins Di–En and Di–Fo (Fig. 3). Even Di_{ss}, which was formed from *pure* Di composition at 1390°C and coexists with glass, has a composition lying between the joins Di–En and Di–Fo. The compositions of the coexisting liquids are also off the join Di–En and lie to the silica side of this join. The tie lines between the coexisting Di_{ss} and the glass are shown in Figure 3. As shown in the figure, the liquid formed from pure Di composition is richer in Wo than pure Di, *i.e.*, pure Di melts incongruently to Di_{ss} with more En than Di and liquid with more Wo than pure Di. This possibility has been shown by Biggar and O'Hara (1969) on the basis of careful quenching experiments near Di compositions and the X-ray powder diffraction method. The probable field of Di_{ss} at the temperature 1390° ± 2°C is shown in Figure 3 on the basis of the present analyses of Di_{ss}. This solid solution range explains the presence of a maximum on the Di_{ss} liquidus found by Kushiro and Schairer (1963) near $Di_{95}Fo_5$ of the join Di–Fo. The maximum on the Fo_{ss}–Di_{ss} liquidus boundary should exist at the intersection of this liquidus boundary and the tie line between Fo_{ss} and the Di_{ss} shown in Figure 3, *i.e.*, to the silica-poor side of the join Di–En.

The melting point of pure Di was measured carefully by Day and Sosman (1910) by the heating-curve method, and the melting point 1391.2° ± 1.5°C (Geophysical Laboratory temperature scale) has been used as a reference point or a secondary standard in many experimental studies. White (1909), however, pointed out that the heating curve of Di does not show a sharp break at the melting point but shows a continuous curvature over a considerable temperature range (>20°). He noted that this phenomenon cannot be easily explained by impurities in Di. However, the observation can be easily explained by incongruent melting behavior of Di. The "melting point" of pure Di, 1391.5°C (the 1948 international temperature scale), should be very close (±1.5°) to the liquidus of the pure Di composition. On the basis of the present study as well as the study by Biggar and O'Hara (1969) pure Di is not the most appropriate substance as a secondary standard of the temperature scale, although its liquidus temperature can still be used as a reference point. $Di_{90}En_{10}$ has a much narrower melting interval (Fig. 4), but it too melts incongruently. Di_{ss} with a composition lying near $Di_{90}En_{10}$ and between the joins Di–En and Di–Fo would melt congruently, although the precise composition of the congruently melting Di_{ss} is not known at present. Single-crystal X-ray examination of this most "stable" Di_{ss}

TABLE 3. Electron Probe Analyses of Coexisting Di_{ss} and Glass Near Di Composition

Starting material		Temperature, °C	Phase	Analyses, weight percent			
Di	En			CaO	MgO	SiO_2	Total
100	0	1390	Di_{ss}	24.88	19.62	54.86	99.36
			Glass	27.52	16.53	54.36	98.41
95	5	1392	Di_{ss}	23.99	20.23	55.09	99.31
			Glass	24.10	19.36	55.07	98.53
85	15	1392	Di_{ss}	22.47	21.35	55.14	98.96
			Glass	21.29	21.72	55.83	98.84
80	20	1391	Di_{ss}	20.82	22.77	55.39	98.98
			Glass	19.54	22.49	56.63	98.66

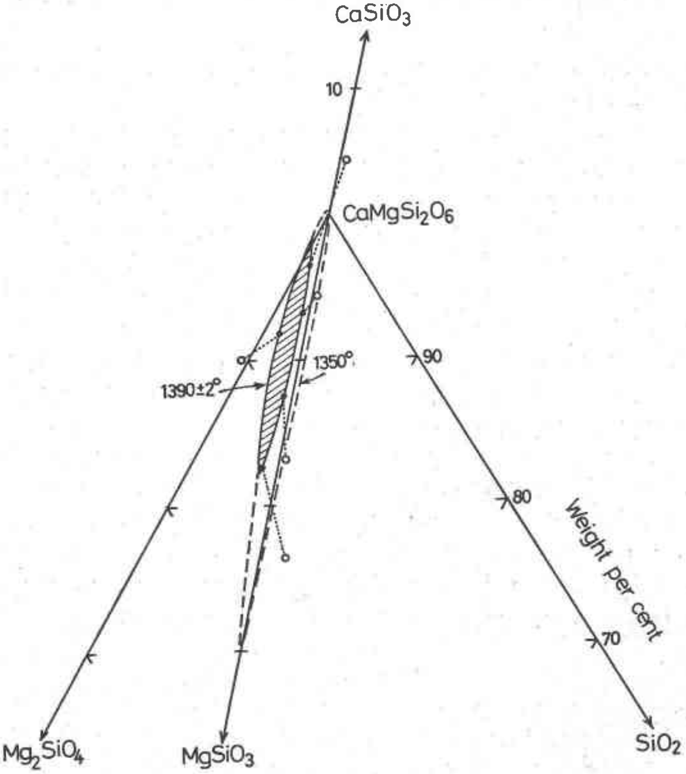

FIG. 3. Probable ranges of Di_{ss} at 1390° ± 2°C and about 1350°C with tie lines between Di_{ss} and liquid at 1390° ± 2°C. Solid circles, compositions of Di_{ss}; open circles, compositions of liquids.

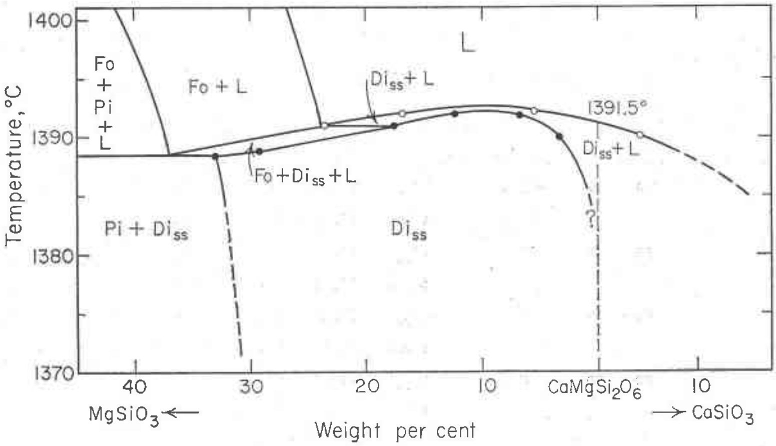

FIG. 4. Equilibrium diagram near Di composition of the join $CaSiO_3$–$MgSiO_3$ at 1 atm, showing incongruent melting of pure Di as well as Di_{ss}.

which has a small amount (less than 5 weight percent) of Fo component, would be very interesting.

The Di_{ss} coexisting with Fo_{ss} and silica-deficient liquid at 1388.5°C also has a composition off the join Di–En (Table 2) and is plotted to the Fo side of the join Di–En (Figs. 1 and 3). This possibility has already been suggested by Kushiro and Schairer (1963).

The present study confirms most of the previous liquidus relations reported or suggested by Schairer and Yoder (1962), Kushiro and Schairer (1963), and Boyd and Schairer (1964) and gives significant additional information on the liquid–crystal relations and the solid solution ranges of the solid phases. The revised liquidus relations can be applied to low-pressure crystallization of basaltic magmas (for example, Mauna Loa and Kilauea lavas described by Macdonald, 1949; Tilley, 1960, 1961; Tilley and Scoon, 1961; and the Muskox intrusion described by Irvine and Smith, 1967). The results can also be applied to the crystallization of pyroxenes, particularly of Ca-poor pyroxenes. Detailed discussion of these problems in the light of the revised system Fo–Di–SiO_2 will be presented elsewhere.

ACKNOWLEDGEMENTS

The present study was greatly facilitated by the earlier works of the late Dr. J. F. Schairer and Drs. F. R. Boyd and H. S. Yoder, Jr., to whom the author is most grateful. The author thanks Drs. H. S. Yoder, Jr., F. R. Boyd, R. N. Thompson, and G. M. Biggar for their comments and critical reading of the manuscript, and Mr. C. G. Hadidiacos for advice concerning the electron probe analysis.

References

Bence, A. E., and A. L. Albee (1968) Empirical correction factors for the electron microanalysis of silicates and oxides. *J. Geol.* **76**, 382–403.

Biggar, G. M., and M. J. O'Hara (1969) Solid solutions at atmospheric pressure in the system CaO–MgO–SiO_2 with special reference to the instabilities of diopside, akermanite and monticellite. *Progress in Experimental Petrology,* Natur. Environment Res. Counc., *First Rep.,* Manchester: Edinburgh, 86–96.

Bowen, N. L. (1912) The binary system: $Na_2Al_2Si_2O_8$ (nephelite, carnegieite)–$CaAl_2Si_2O_8$ (anorthite). *Amer. J. Sci.* **33**, 551–573.

——— (1914) The ternary system diopside–forsterite–silica. *Amer. J. Sci.* **38**, 207–264.

Boyd, F. R. (1968) Quantitative electron–probe analysis of pyroxenes. *Carnegie Inst. Wash. Year Book,* **66**, 327–334.

——— (1970) Garnet peridotites and the system $CaSiO_3$–$MgSiO_3$–Al_2O_3. *Mineral. Soc. Amer. Spec. Pap.* **3**, 63–75.

———, and J. F. Schairer (1964) The system $MgSiO_3$–$CaMgSi_2O_6$. *J. Petrology,* **5**, 545–560.

Day, A. L., and R. B. Sosman (1910) The nitrogen thermometer from zinc to palladium. *Amer. J. Sci.* **29**, 93–161.

Finger, L. W., and C. G. Hadidiacos (1971) Aspects of computer automation of an electron microprobe. *Carnegie Inst. Wash. Year Book,* **70**, 269–275.

Irvine, T. N., and C. H. Smith (1967) The ultramafic rocks of the Muskox intrusion, Northwest Territories, Canada. In P. J. Wyllie, ed., *Ultramafic and Related Rocks,* John Wiley & Sons, Inc. New York, 38–49.

Kushiro, I. (1969) The system forsterite–diopside–silica with and without water at high pressures. *Amer. J. Sci.,* **267–A**, 269–194.

———, and J. F. Schairer (1963) New data on the system diopside–forsterite–silica. *Carnegie Inst. Wash. Year Book,* **62**, 95–103.

———, and H. S. Yoder, Jr. (1970) Stability field of iron–free pigeonite in the system $MgSiO_3$–$CaMgSi_2O_6$. *Carnegie Inst. Wash. Year Book,* **68**, 226–229.

Macdonald, G. A. (1949) Hawaiian petrographic province. *Geol. Soc. Amer. Bull.* **60**, 1541–1596.

Schairer, J. F., and H. S. Yoder, Jr. (1962) The system diopside–enstatite–silica. *Carnegie Inst. Wash. Year Book,* **61**, 75–82.

———, and I. Kushiro (1964) The join diopside–silica. *Carnegie Inst. Wash. Year Book,* **63**, 130–132.

Tilley, C. E. (1960) Differentitation of Hawaiian basalts: Some variants in lava suites of dated Kilauean eruptions. *J. Petrology,* **1**, 47–55.

——— (1961) The occurrence of hypersthene in Hawaiian basalts. *Geol. Mag.* **98**, 257–260.

———, and J. H. Scoon (1961) Differentiation of Hawaiian basalts: Trends of Mauna Loa and Kilauea historic magma. *Amer. J. Sci.* **254**, 60–68.

White, W. P. (1909) Melting point determination: Melting point methods at high temperatures. *Amer. J. Sci.* **28**, 453–489.

Yang, Houng-Yi (1971) Synthesis of the iron–free pigeonite at atmospheric pressure. *Geol. Soc. Amer., Abstr. Progr.* **3**, 759–760.

Manuscript received, February 7, 1972; accepted for publication, March 28, 1972.